applied sciences

MDPI

Case Report

Deep Learning-Based Approach for Optimizing Urban Commercial Space Expansion Using Artificial Neural Networks

Dawei Yang [1,*], Jiahui Zhao [1] and Ping Xu [2]

[1] Civil &Architecture Engineering, Xi'an Technological University, Xi'an 710021, China
[2] Urban Renewal Research Institute, Shaanxi Institute of Urban and Rural Planning and Design, Xi'an 710033, China
* Correspondence: yangdawei@xatu.edu.cn

Abstract: Amid escalating urbanization, devising rational commercial space layouts is a critical challenge. By leveraging machine learning, this study used a backpropagation (BP) neural network to optimize commercial spaces in Weinan City's central urban area. The results indicate an increased number of commercial facilities with a trend of multi-centered agglomeration and outward expansion. Based on these findings, we propose a strategic framework for rational commercial space development that emphasizes aggregation centers, development axes, and spatial guidelines. This strategy provides valuable insights for urban planners in small- and medium-sized cities in the Yellow River Basin and metropolitan areas, ultimately showcasing the power of machine learning in enhancing urban planning.

Keywords: commercial space; points of interest; deep learning; BP neural network

Citation: Yang, D.; Zhao, J.; Xu, P. Deep Learning-Based Approach for Optimizing Urban Commercial Space Expansion Using Artificial Neural Networks. *Appl. Sci.* **2024**, *14*, 3845. https://doi.org/10.3390/app14093845

Academic Editor: Douglas O'Shaughnessy

Received: 22 March 2024
Revised: 23 April 2024
Accepted: 26 April 2024
Published: 30 April 2024

1. Introduction

The rapid global urbanization, which is projected to exceed 60% by 2030, is leading to profound adjustments in cities' industrial structures and posing challenges to urban development. As cities adapt to these transformations, the role of commercial activities in reshaping urban space becomes increasingly significant. A well-designed commercial area not only fuels economic development but also meets residents' consumption needs while enhancing their comfort and happiness. Therefore, it is of utmost importance to simulate and optimize the expansion of urban commercial space for effective urban planning.

Effective commercial areas integrate diverse facilities and services that are accessible and beneficial to the community, contributing to vibrant urban life. Therefore, the simulation and optimization of urban commercial space expansion are essential for strategic urban planning. This process helps planners and developers to predict and respond to the dynamic needs of urban populations, ensuring that commercial developments are sustainable, equitable, and conducive to economic prosperity.

In light of these challenges, it is crucial to develop tools and methodologies that can accurately model and optimize commercial space layouts in urban settings. The integration of advanced technologies, such as artificial intelligence and geographic information systems, into urban planning processes allows for more precise and efficient planning. By utilizing data-driven approaches, urban planners can create more adaptive and responsive urban environments that not only meet current needs but are also scalable for future demands.

In a rapidly changing world, understanding the significance of commerce in cities goes beyond economic prosperity; it is about shaping livable and business-friendly urban environments that create more opportunities and benefits for residents. Through in-depth research and comprehensive analysis, we can discover that a rational layout of commercial space not only promotes sustainable urban development but also strengthens community cohesion and improves residents' quality of life.

Through rigorous, in-depth research and comprehensive analysis, urban planners and developers can uncover the profound impacts that a well-thought-out commercial space layout has on a city's overall ecosystem. A rational layout of commercial spaces not only boosts sustainable urban development by making efficient use of land and resources but also plays a crucial role in enhancing community cohesion. Such planning ensures that commercial areas are accessible, culturally inclusive, and economically viable, which, in turn, fosters a sense of belonging among residents.

The planning and development of commercial areas must take a holistic approach that prioritizes social and environmental sustainability. This involves not just the integration of innovative architectural designs and diverse commercial offerings but also a commitment to creating spaces that foster community engagement and support the local economy. By emphasizing innovation and diversity, urban planners can provide cities with a broad spectrum of choices and opportunities that cater to a variety of tastes and needs. The variety not only enriches the urban experience but also attracts a diverse array of visitors and residents, enhancing the city's cultural fabric and economic vitality.

Therefore, research on the effective planning and optimization of urban commercial space holds significant meaning. It not only drives sustainable urban development but also creates more livable and prosperous urban environments, leading to greater well-being and happiness in people's lives. Effective commercial planning involves strategic site selection, thoughtful design, and the integration of amenities that enhance public life. By focusing on accessibility and human-scale developments, these areas become more than just places of commerce—they become central hubs for community activity and engagement. Optimized commercial spaces can act as catalysts for local economic growth by attracting businesses and investors. Economic stimulation can lead to job creation and provide a wider range of services and products to the community, further boosting the local economy. As commercial areas thrive, they contribute to the overall economic health of the city, creating a virtuous cycle of growth and improvement.

Urban commercial spaces are influenced by a variety of factors, including transportation, policy, economic conditions, and historical context. Traditionally, qualitative analysis methods in urban planning heavily relied on the intuition of planners, often leading to subjective outcomes. However, with the application of artificial intelligence and machine learning, an increasing number of planners are incorporating these complex technologies into urban planning methodologies, marking a significant shift in the field [1–4]. The multidisciplinary approach utilizes extensive data sets and applies systematic rules to continuously refine results. It can effectively solve site selection challenges by simulating the most suitable locations based on key influencing factors [5–7]. Additionally, machine learning techniques can be integrated with image data to further enhance research. The integration helps in identifying image features and facilitates the semantic segmentation of streetscape images, leading to more precise and objective urban planning outcomes [8–11].

Machine learning, when synergistically combined with urban cellular automata (CA) models, has engendered a range of sophisticated CA-based urban simulation models, such as artificial neural network-based cellular automata (ANN-CA) [12,13] and random forest-based cellular automata (RF-CA) [14–16]. These innovative models are pivotal in simulating and predicting the evolution of urban spaces into the future. The increasing application of machine learning in urban commercial spaces signifies a transformative trend aimed at diminishing the inherent subjectivity in urban planning processes.

ANNs are particularly adept at modeling complex and dynamic relationships, making them suitable for predicting various urban dynamics that are non-linear in nature. For instance, ANNs have been successfully applied to predict daily city water consumption—which is a critical component of urban infrastructure management—owing to their capacity to learn and model from vast datasets [17,18]. ANNs are instrumental in functional area classification, where they categorize different urban zones based on usage, such as residential, commercial, or industrial, which is essential for effective urban planning and resource allocation [19]. Decision trees facilitate the understanding and visualization of data through

a tree-structured classifier, where decisions are made and outcomes are predicted based on the data attributes. In urban planning, decision trees have been utilized to discern correlations between the physical attributes of buildings and the socio-economic levels of inhabitants. This application is vital as it aids urban planners and policymakers in identifying and implementing targeted interventions aimed at improving living conditions and planning new developments [20]. Support vector machines (SVMs) are robust classifiers that work well on both linear and non-linear problems. They are particularly effective in classifying complex urban data into predefined categories and have been integrated with geographic information systems (GISs) for enhanced spatial analysis [21–23]. This integration is crucial for applications such as predicting landslide susceptibility in urban and peri-urban areas, thereby enabling preventive planning and mitigation strategies to enhance urban resilience.

ANNs have been specifically selected to simulate the expansion of urban commercial spaces [24–27]. The choice is predicated on the ANNs superior ability to handle and model complex relationships within large datasets, thereby facilitating more effective optimization and planning of commercial space distribution. The employment of ANNs supports the creation of more rational, data-driven urban planning processes, ultimately leading to better decision-making by urban planners. The strategic application not only optimizes commercial space allocation but also contributes significantly to the broader goals of sustainable urban development, enhancing the overall functionality and livability of urban environments.

Within the vast field of ANNs, there exists a wide variety of models, each tailored to specific types of data and prediction needs. Notable among them are radial basis function (RBF) networks, Elman networks, and backpropagation (BP) neural networks, each of which serves a different purpose and demonstrates unique functionality and plays an important role in urban, social, and engineering fields [28–36].

RBF networks are a type of neural network that uses radial basis functions as activation functions [37,38]. They are particularly known for their effectiveness in handling non-linear data separations [39–41]. RBF networks have been extensively applied in urban planning contexts, particularly in predicting urban commercial and industry land demand [42–44]. Their ability to interpolate surfaces or spaces makes them exceptionally suitable for modeling complex urban growth patterns, thus aiding in the planning and development of smart cities.

Elman networks are well suited to capturing dynamic changes over time, making them ideal for applications involving temporal sequences [45]. In the realm of environmental science, Elman networks have been effectively utilized to predict carbon emissions and monitor changes in average sea levels [46]. Their recurrent nature allows them to perform well in scenarios where data points are temporally connected, providing planners and environmentalists with a powerful tool for assessing long-term environmental impacts and trends [47].

BP networks have gained widespread acclaim for their robustness and adaptability across a diverse array of predictive modeling tasks. These networks are particularly lauded for their layered architecture, which allows for the meticulous modeling of complex relationships between input and output variables. The efficacy of BP networks in error correction via the backpropagation algorithm is unparalleled, rendering them exceedingly proficient in unraveling multifaceted problems in predictive analytics [48,49]. In the domain of urban planning, the application of BP neural networks has been particularly transformative [50]. Urban planners have harnessed these networks to forecast urban air quality indices with remarkable accuracy, taking into account multifarious variables, such as traffic flow, industrial emissions, and meteorological data [51,52]. This predictive capacity is instrumental in the development of urban policies aimed at air quality management and the mitigation of health risks associated with airborne pollutants.

Furthermore, BP neural networks have been adeptly utilized to assess and predict regional flood hazards. These networks analyze vast datasets, including topographical

maps, hydrological patterns, and historical flood data, to predict potential flood zones with high precision [53]. This information is crucial for urban developers and policymakers to plan strategically placed flood defenses, implement effective drainage systems, and delineate land use that minimizes flood risk. BP networks extend to the spatial configuration of urban landscapes as well. By analyzing data on population density, land use, and socioeconomic activities, these networks support the optimization of urban space allocation, facilitating the creation of well-balanced, sustainable urban environments [54]. BP networks assist urban planners in the intelligent design of urban spaces that harmoniously integrate residential areas with commercial, recreational, and green spaces, contributing to the socioeconomic dynamism and environmental resilience of urban centers. In conclusion, the implementation of BP neural networks within the scope of urban spatial planning and development underlines a significant advancement in the field, marrying the analytical rigor of machine learning with the strategic vision of urban development [55]. This synergy is pivotal for crafting smart cities that are both sustainable and conducive to an enhanced quality of urban life.

Despite the distinct benefits offered by RBF and Elman networks, backpropagation (BP) networks are exceedingly prominent in the field, representing a significant majority of neural network applications across a range of disciplines [56–61]. Their widespread adoption is attributed to their comprehensive applicability and proven effectiveness in addressing complex predictive modeling tasks [62–70]. The dominance is attributed to the BP network's flexible architecture, which can be adjusted and scaled according to the complexity of the task at hand, making it a versatile tool for many predictive tasks.

This study chose to employ a BP neural network to simulate the expansion of urban commercial space. This decision was based on the network's proven track record in handling complex datasets and its ability to model intricate relationships within urban planning data. This approach ensured that the predictions made were both reliable and relevant, providing urban planners with a robust tool for making informed decisions that are critical for sustainable urban development. This methodology not only enhanced the accuracy of the urban space modeling but also contributed to more effective and efficient urban planning and development processes.

In the subsequent sections of this paper, we explore the methodologies employed, including a detailed explanation of the data collection process and the machine learning techniques applied. We then delve into the results and discussion, where the outcomes of our analyses are presented and interpreted in the context of existing literature. Finally, our conclusions summarize the implications of our findings and suggest directions for future research, highlighting how this study contributes to the broader field of urban commercial space.

2. Study Area and Data

2.1. Study Area

This study concentrated on the Linwei District of Weinan City, which is located in the east-central part of Shaanxi Province, China, strategically situated on the main axis of the Guanzhong–Tianshui Economic Zone. Linwei District is a pivotal area, as delineated by the city's comprehensive Urban Master Plan for the years 2016 to 2030, and Weinan City is an important city in the Golden Triangle demonstration zone in the Yellow River, which is a regional planning zone in China. To the east are Sanmenxia City and Yuncheng City in Henan Province, to the west are Tongchuan City, Xianyang City, and Xi'an City (the capital of Shaanxi Province and an important city in western China), and to the south is Shangluo City in Shaanxi Province. Weinan City spans an extensive area of 13,134 km^2, making it the largest city in the province, with a predominant focus on agriculture. The significance of Linwei District within the urban landscape is underscored by its substantial economic contribution. As of 2020, with its population of 920,000, the district accounted for an impressive 23.68% of Weinan City's gross domestic product (GDP). This notable figure not only highlights Linwei District's role in fueling the city's economic engine but

also cements its status as the central commercial nexus. The district's robust economic performance, marked by such a notable share in the city's GDP, underscores its critical function as an economic powerhouse and a focal point for both commerce and development within the region (Figure 1).

Figure 1. The district of Weinan City.

This study was centered on Linwei District for five reasons. First, Weinan City is experiencing a significant developmental phase, and with the commercial space in Linwei District expected to undergo substantial expansion, accurate forecasting and simulation become critical to achieving a strategically distributed commercial layout. The growth in the city's GDP and retail sales accentuates the urgency of the planning. Second, Weinan City's strategic proximity to the metropolis of Xi'an, coupled with its burgeoning commercial activity, positions it as an exemplar for urban commercial development. Its lessons and models hold significant relevance for smaller- and medium-sized neighboring cities, particularly those on the fringe of larger metropolitan zones. Third, Linwei District is representative of the transformative effects of infrastructural investments on urban development. The district has witnessed a surge in such investments, which have catalyzed local economic activities and urban revitalization. This case study provided a unique opportunity to analyze the impact of infrastructure on commercial space distribution and urban economic health. Fourth, this district served as a microcosm for studying the integration of traditional agricultural economies with modern commercial expansion. This interplay is crucial for understanding how rapidly urbanizing regions can balance heritage with progress, making Linwei District an ideal candidate for in-depth research into sustainable urban commercial growth that respects and incorporates its agricultural roots. Lastly, the data accessibility within China, which facilitated a thorough and detailed analysis of urban growth patterns and commercial development strategies.

2.2. Study Data

This study utilized four primary data types: traditional data, geographic data, network data, and image data. Traditional data comprised statistical yearbooks, development bulletins, and city master plans from Weinan City's government units. Geographic data were mainly sourced from the National Geographic Information Resources Catalogue Service System (www.webmap.cn, accessed on 12 July 2022), while network data included point of interest (POI) data from www.amap.com and OSM road network data from Open Street Map (www.openstreetmap.com, accessed on 12 July 2022). Image data consisted of street view photos from Linwei District. For efficiency, these data were organized,

calibrated, and integrated into Arc GIS 10.4, with the final coordinate system unified to WGS_1984_UTM_Zone_53N.

POI data were the most important data for this study, as it encapsulated the vital locations that defined the functionality and vibrancy of urban life within the Linwei District. These data were critical because it provided insights into the distribution and diversity of services, amenities, and infrastructures. The acquisition of POI data was executed through advanced Python scripts utilizing the requests and json libraries, which enabled the dynamic collection of data from Amap's location service APIs for the periods of 2023. Linwei District POI data contained 44,034 points (Figure 2). There were eight categories, of which administration had a total of 6399 data, business had a total of 22,886 data, education had a total of 2088 data, medical had a total of 2465 data, office had a total of 3609 data, residential had a total of 2256 data, tourism had a total of 192 data, and traffic had a total of 4139 data. All data were disseminated through the website.

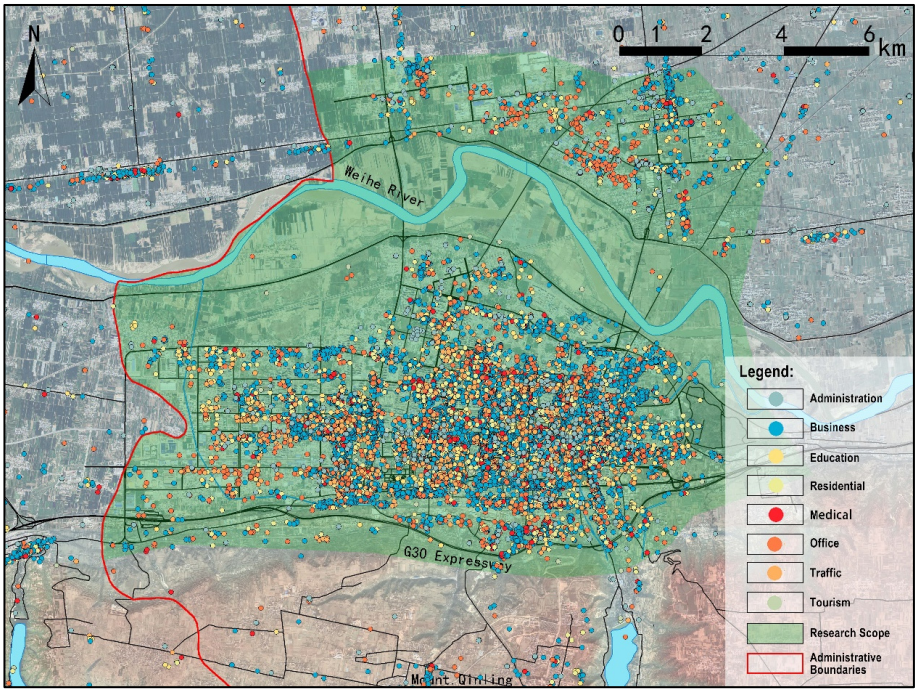

Figure 2. POI data diagram.

3. Methods

3.1. Backpropagation Neural Network

Data visualization within this study was meticulously carried out using ArcGIS 10.4, which provided an intuitive platform for mapping and analyzing the geographical distributions of data points. Concurrently, data analysis and model optimization tasks were conducted using Python, which is a versatile programming language known for its robust libraries and frameworks that support complex data analysis and machine learning algorithms (Figure 3).

In the realm of neural networks, the BP neural networks employed here were typically structured with three layers: the input layer, the hidden layer, and the output layer. Each node in the hidden layer was equipped with an activation function, which was crucial for the network's ability to capture non-linear relationships within the data. The use of BP neural networks in this study was pivotal due to their proficiency in handling multilayered learning processes, which was essential for the complex nature of urban data. The choice to utilize a three-layer BP neural network structure was driven by the need for a balance between simplicity and computational efficiency. A three-layer architecture provided sufficient complexity to model non-linear relationships and interactions between variables,

facilitating a clear understanding of how inputs influence outputs, which is essential for practical applications in urban planning. The simplicity aided in maintaining model transparency and interchangeability, which are crucial for stakeholders who depend on the clarity of model findings. Additionally, more complex multi-layer networks increase the risk of overfitting, where a model learns the noise in the training data rather than the actual patterns, leading to poor performance on new, unseen data. A simpler three-layer network mitigates the risk and requires less computational power and time to train, which is vital given the large datasets typically involved in urban studies. Furthermore, adhering to the principle of parsimony, or Occam's razor, suggests selecting the simplest model that sufficiently captures the underlying trends. This approach not only ensures a more robust and generalized model but also aligns with empirical evidence that often finds three-layer networks are adequate for effectively modeling complex phenomena.

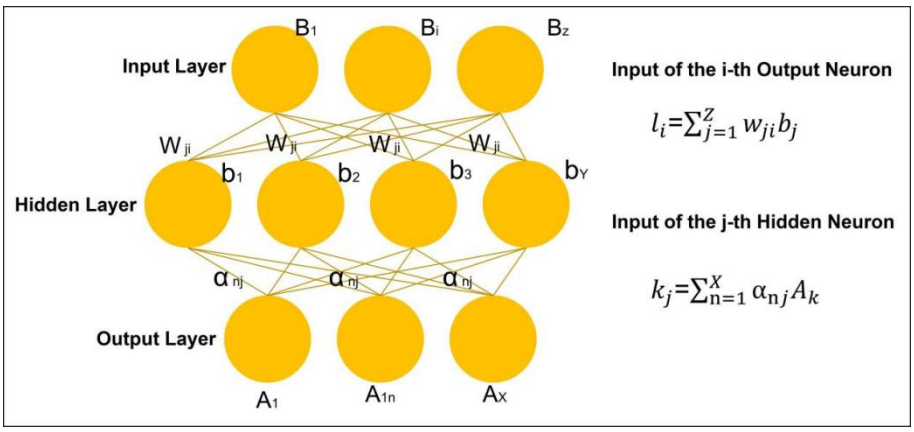

Figure 3. BP neural network algorithm diagram.

The operational flow of the BP neural network algorithm implemented in research includes several critical steps designed to optimize the accuracy and reliability of the model predictions. These steps are detailed as follows:

Identification and normalization of feature values: Initially, relevant feature values were identified from the dataset, which involved selecting significant variables that influenced the study outcomes. Subsequently, all data underwent normalization to ensure that the neural network processed values on a comparable scale, which was fundamental for achieving model stability and convergence during training.

Parameter setting for network training: After normalizing the data, the parameters of the BP neural network, such as the number of neurons in each layer, the learning rate, and the activation functions, were meticulously established. These parameters were crucial, as they directly influenced the learning efficiency and the predictive performance of the network.

Simulation and output evaluation: With the parameters set, the neural network was trained on the data, and model predictions were generated. The output from the neural network was then critically assessed against predefined accuracy metrics. If the output met the set accuracy standards, a reverse normalization process was applied to transform the data back to its original scale, facilitating the practical interpretation and application of the results.

The methodical approach to data visualization, analysis, and neural network training ensured that the study not only adhered to rigorous scientific standards but also yielded actionable insights that could significantly influence urban planning and policy-making.

The BP algorithm is shown in Figure 3, which was actually given a training set $X = \{(A_k, B_k)\}_{k=1}^{n}$ to determine the X input neurons, Y output neurons, and Z output neurons, where the threshold of neurons in the output layer is denoted by θ_i, the threshold of neurons in the hidden layer is denoted by μ_j, the connection weights between the input layer and hidden layer neurons are α_{nj}, and the connection weights between the

hidden layer and output layer neurons are ω_{ji}. The input of the hidden layer neuron is $k_j = \sum_{n=1}^{x} a_{nj} A_k$, and the input of the output layer neuron is $l_i = \sum_{j=1}^{Z} w_{ji} b_j$, where b_j is the hidden layer neuron output, assuming that both the hidden layer and output layer neurons used the sigmoid function. For the training set, the output of the neuron was

$$\hat{B}_l^k = f(l_i - \theta_i) \tag{1}$$

where $f(l_i - \theta_i)$ is the sigmoid function and the net i is the input to the neuron. The mean square error (MSE) over the network is given by

$$E_k = \frac{1}{2} \sum_{i=1}^{Y} \left(\hat{A}_i^k - A_i^k \right) \tag{2}$$

where $\hat{A}_i^k$ is the target output and A_i^k is the actual output of the network.

The BP neural network utilized an iterative approach to minimize the MSE through the adjustment of weights and thresholds. This was done by updating the parameters using the following general formula for each iteration:

$$\vartheta \longleftarrow \vartheta + \Delta\vartheta \tag{3}$$

$$\Delta w_{ji} = -\eta \frac{\partial E_k}{\partial w_{ji}} \tag{4}$$

$$\frac{\partial E_k}{\partial w_{ji}} = \frac{\partial E_k}{\partial \hat{B}_i^k} \times \frac{\partial \hat{B}_i^k}{\partial l_i} \times \frac{\partial l_i}{\partial w_{ji}} \tag{5}$$

And

$$\frac{\partial l_i}{\partial w_{ji}} = b_j \tag{6}$$

where Δ represents the changes made to each parameter. Given the sigmoid activation function, the derivative used in the backpropagation was

$$f'(x) = f(x)(1 - f(x)) \tag{7}$$

Combining Equations (1) and (2) during the backpropagation phase, the weight updates could be computed as follows:

$$g_k = -\frac{\partial E_k}{\partial \hat{B}_i^k} \times \frac{\partial \hat{B}_i^k}{\partial l_i} = -\left(\hat{B}_l^k - B_l^k \right) f'(l_i - \theta_i) = \hat{B}_l^k \left(1 - \hat{B}_l^k \right) \left(\hat{B}_l^k - B_i^k \right) \tag{8}$$

Collating all these equations from (1) to (8) helped in systematically updating the model's parameters during training, ensuring the model effectively learned from the training data.

$$\Delta w_{ji} = \eta g_k b_j \tag{9}$$

where η is the learning rate. The same reasoning applies to obtain

$$\Delta\theta_i = -\eta g_k \tag{10}$$

$$e_j = -\frac{\partial E_k}{\partial l_i} * \frac{\partial l_i}{\partial K_i} = -\sum_{k=1}^{Y} \frac{\partial E_k}{\partial l_i} * \frac{\partial l_i}{\partial b_j} f'(k_j - \mu_j) = b_j (1 - b_j) \sum_{k=1}^{Y} w_{ji} * g_k \tag{11}$$

$$\Delta\alpha_{nj} = \eta e_j X_n \tag{12}$$

$$\Delta\mu_j = -\eta e_j \tag{13}$$

The reasoning extended similarly for biases and weights throughout the network, systematically updating each according to the error correction calculated at each step of the learning process. All the formulas of the BP neural network were programmed in Matlab.

3.2. Eigenvalue Selection

The study area was segmented into unique square cells based on the range of a five-minute living circle. Each cell was assigned a unique number, which enabled the spatial correlation of the POI data. The POI data were sorted into eight functional categories: tourism, medical, science and education, commercial, administrative, office, transportation, and residential. Using the "spatial connection" tool in ArcGIS 10.4, each POI datum was linked with spatially co-located cells, which allowed for the counting of each functional POI in each cell.

The statistical distribution of the POI data indicates a correlation between commercial POI and other functional POI. The Pearson product-moment correlation coefficient analysis reveals a positive correlation when the coefficient is above 0, with values closer to 1 being stronger.

Based on the above, the commercial POI data generally showed high positive correlation (>0.5) with seven categories (transportation, office, residential, administrative, scientific, educational, and medical), implying a mutual influence in their numbers. Notably, the office function had a high correlation of 0.82 with the commercial function. In contrast, tourism showed a weak correlation (~0.2) with other functions, indicating minimal influence.

Consequently, the seven functions that demonstrated strong correlations were selected as characteristic variables for further analysis and modeling within the study, highlighting their importance in understanding the dynamics of urban commercial spaces.

3.3. Parameter Debugging

(1) Number of nodes per layer

Increasing the number of neuron nodes generally enhances the training effectiveness of BP neural networks, effectively reducing the overall error in predictions (Figure 4). In practical applications, the quantity of nodes is typically iteratively adjusted to optimize network performance. In this case, after conducting 250 trials to refine the model, the optimal network configuration was established as having 50 nodes in the input layer, 90 nodes in the hidden layer, and 90 nodes in the output layer. The specific configuration demonstrated robust performance, achieving an R^2 score of 0.7719 and a remarkably low error rate of 0.0015, indicating a high degree of predictive accuracy and model reliability.

(2) Learning rate and momentum

The learning rate is a critical parameter in neural networks that directly influences the magnitude of weight adjustments during training. Both excessively high and low learning rates can negatively impact the performance of a backpropagation (BP) neural network, leading to either erratic or insufficient updates to the model's weights. Similarly, the momentum parameter plays a pivotal role in determining the consistency of the gradient's direction across updates, enhancing the training process when consistent and moderating updates otherwise. In our experiments, we conducted multiple tests on the BP neural network, varying the momentum between 0.1 to 0.9 and adjusting learning rates from 0.01 to 0.1. Through these tests, we identified that the network achieved an optimal performance with a momentum of 0.5 and a learning rate of 0.04, resulting in an R^2 score of 0.7688 (Figure 5). This combination of learning rate and momentum was shown to be the most effective in achieving a balance between the rapid convergence and stability of the learning process. The learning rate, which is a crucial neural network parameter, influences the weight changes' magnitude. Both overly high and low learning rates adversely affect the BP neural network. The momentum determines the consistency of the gradient direction, boosting updates if consistent and reducing them otherwise. Multiple tests were conducted on our BP neural network, with the momentum varying from 0.1 to 0.9 and learning rates from 0.01 to 0.1. The optimal result with an R^2 score of 0.7688 was achieved at a momentum of 0.5 and a learning rate of 0.04.

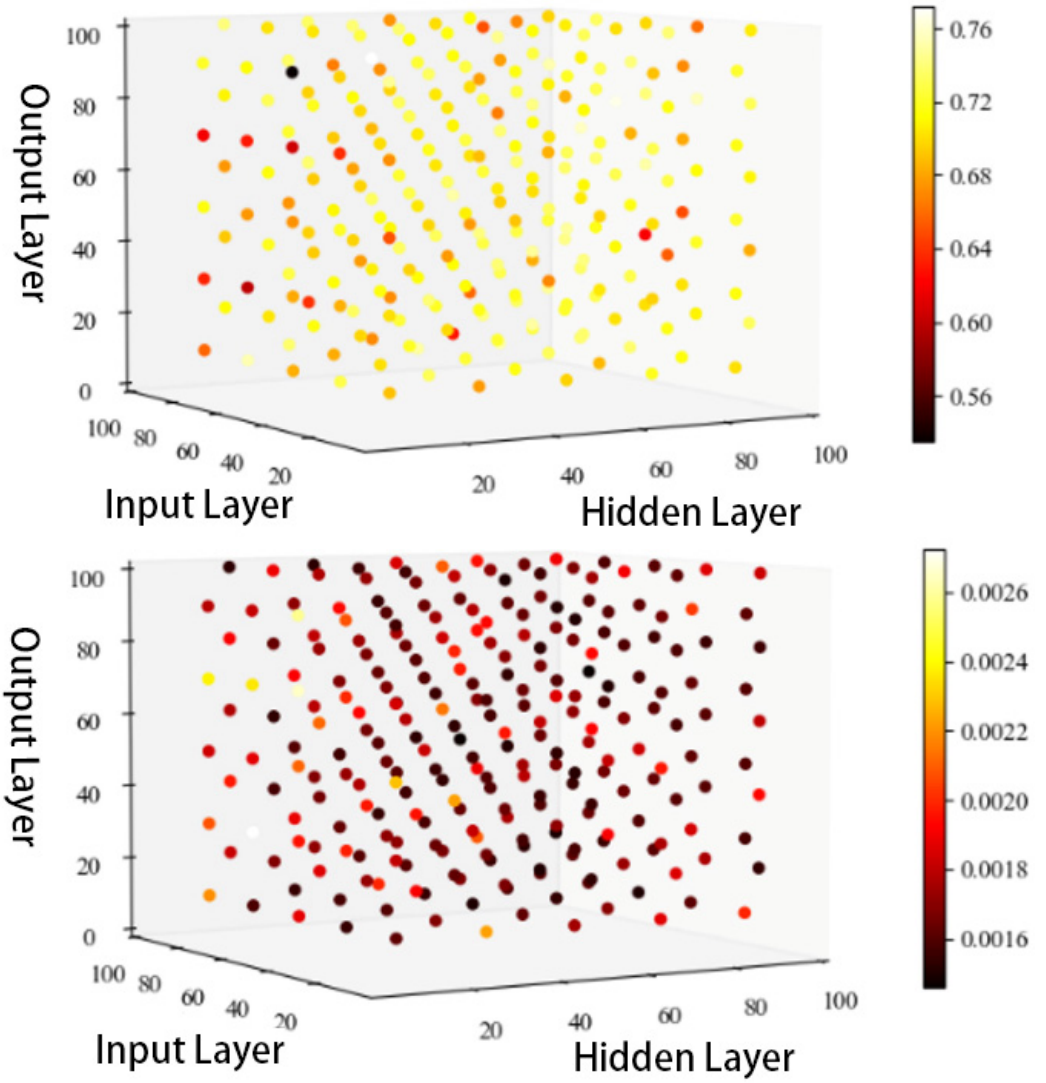

Figure 4. R^2 score and error of neurons in each layer.

(3) Excitation function

In BP neural networks, excitation functions are utilized for non-linear processing. While the output layer typically uses sigmoid as the default, this study tested various combinations of excitation functions. After nine trials, the optimal configuration was identified as tanh for the input layer and sigmoid for the output layer. This combination yielded an R^2 score of 0.6952 and an error of 0.0018 (Table 1).

Table 1. R^2 score and error of excitation function.

Input Layer	Hidden Layer	Error	R^2
Sigmoid	Sigmoid	0.006195	0.0238
Sigmoid	Rule	0.003329	0.4171
Sigmoid	Tanh	0.002153	0.6487
Rule	Sigmoid	0.002409	0.5743
Rule	Rule	0.002267	0.5972
Rule	Tanh	0.001976	0.6877
Tanh	Sigmoid	0.003035	0.5906
Tanh	Rule	0.001943	0.6917
Tanh	Tanh	0.001840	0.6952

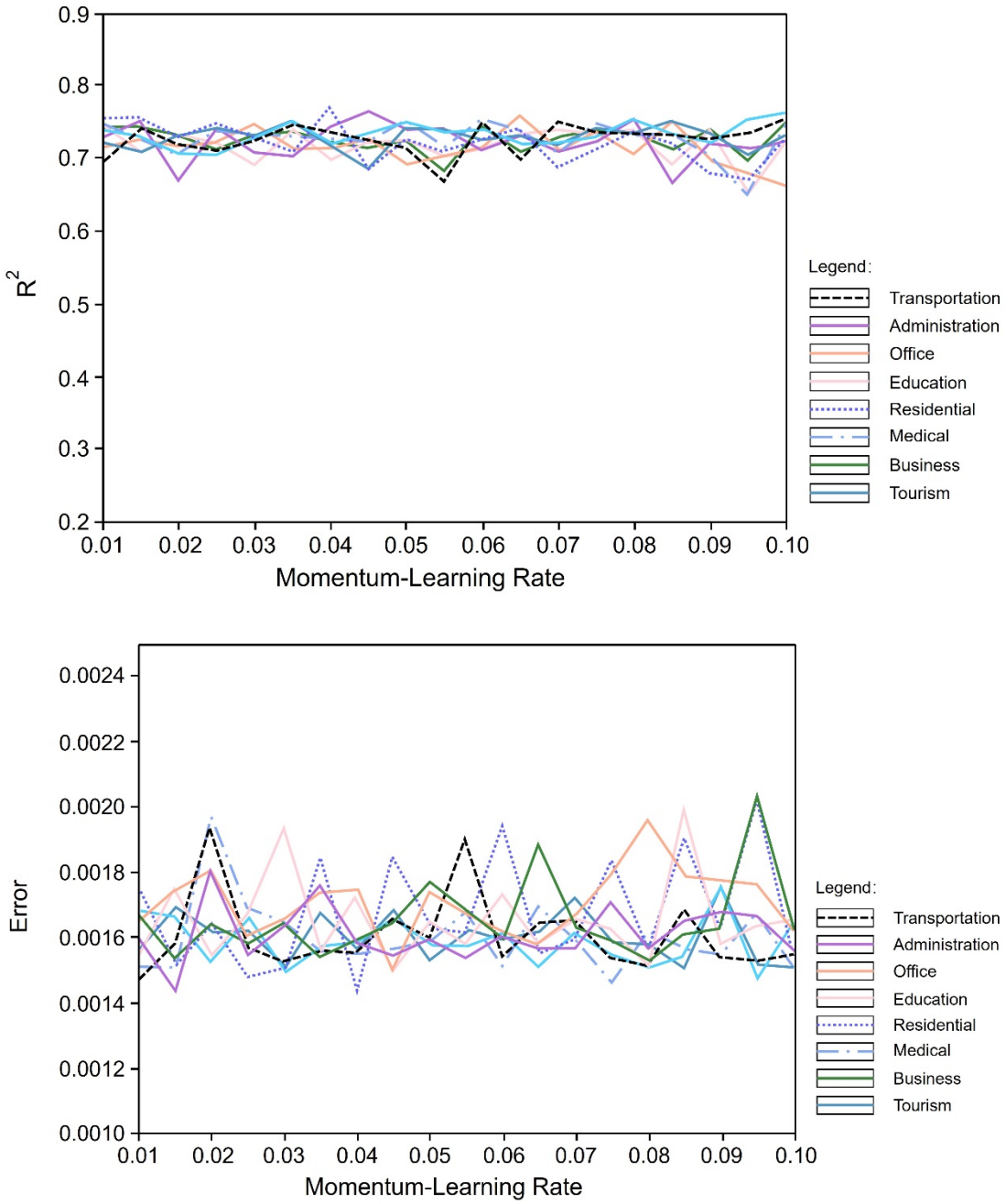

Figure 5. R^2 score and error line in momentum-learning rate.

4. Discussion

4.1. Model Prediction and Output

To avoid an overlap between the training and prediction sets, the algorithm employed a ten-fold cross-validation, which partitioned the data into ten subsets, each in turn serving as a validation set while the remainder formed the training set. This approach reduced the bias and prevented the training set from coincidentally resembling the data condition, enhancing the reliability of the learning outcomes.

The BP neural network optimization model used the number of commercial POI facilities in each grid as the dependent variable and other functional POI facilities as independent variables.

The research adopted a grid-based approach, selecting square grids as the focal point of study due to the convenience they offerred in conducting spatial analysis and the reliability they provided in terms of data support. The study area was methodically subdivided into

a grid of 1 km × 1 km squares using the fishing net tool, resulting in a comprehensive total of 1097 individual units for a detailed analysis. This resulted in an optimized commercial facility with an R^2 = 0.7046, and an increase in the total number of commercial facilities from 44,034 to 49,871.

Figure 6 displays the static density map of both the existing and optimized commercial spaces, with the density of commercial facilities in each cell indicated. The optimization results, which were categorized and visualized by the same criteria, were exported to the field properties in the ArcGIS software. This revealed a prospective development of commercial space in Weinan City's center, which was focused around two agglomeration points in a multi-core pattern, with commercial complexes propelling the growth. Such a spatial representation not only encapsulated the current state but also forecasted the evolution of commercial zones, signifying where growth is likely to intensify.

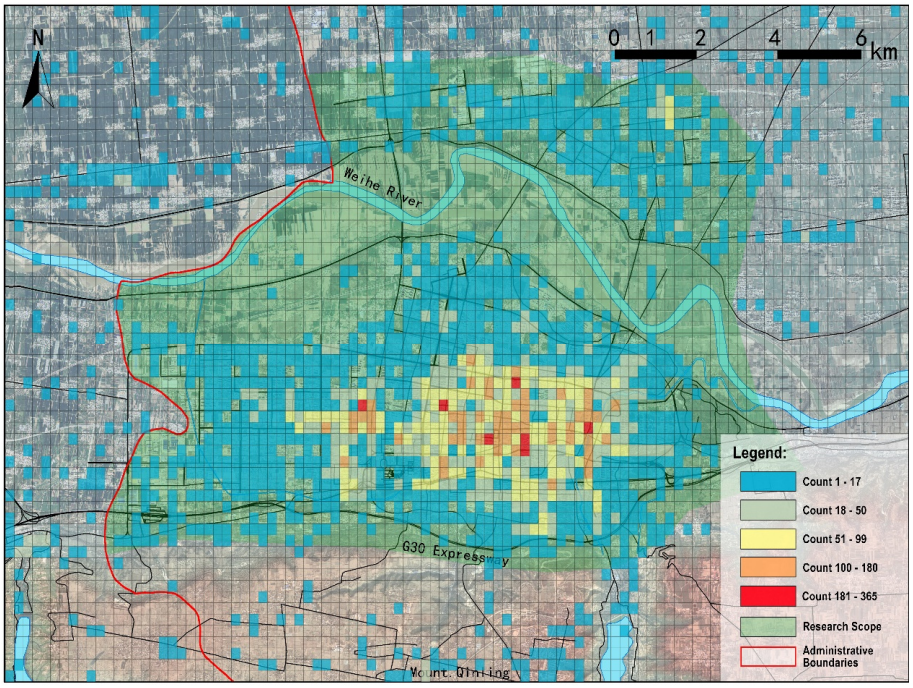

Figure 6. Static density variation diagram.

The envisioned commercial expansion, as it unfurls along the main transportation routes, commands a wider influence than the currently observed commercial footprint. Significant developments are poised to stretch westward into the dynamic high-tech industrial development zone, as well as northward, bridging the river into the economic and technological development zone, reflecting strategic foresight in urban commercial growth.

Figure 7 deftly superimposes the projected commercial facilities upon the existing commercial landscape, spotlighting the strategic areas of Chaoyang Street and Lotian Street at the heart of Weinan City's center. Chaoyang Street is already home to sizable commercial complexes, whereas Lotian Street, despite its paucity of large-scale commercial entities, demonstrates a dense congregation of commercial activity.

These observations are astutely aligned with the principles of traditional agglomeration theory and central place theory. Chaoyang Street and Lotian Street are identified as nascent hubs of urban commerce, with Chaoyang Street already exhibiting a pronounced degree of commercial clustering. The forecasted growth in commercial space dovetails with the optimized projections, thereby affirming the validity of agglomeration tendencies and central place theory within the urban planning context.

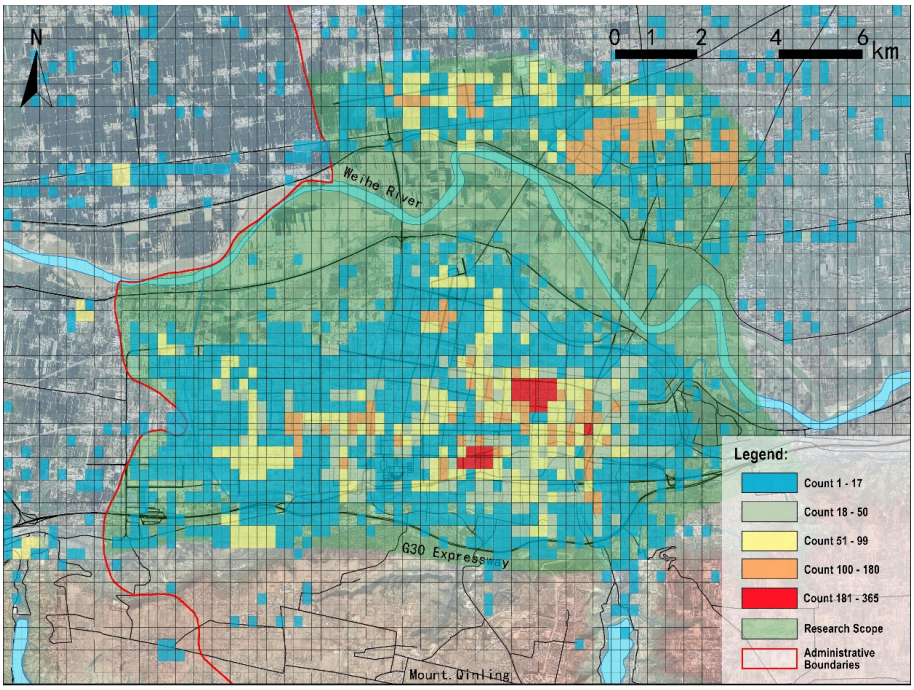

Figure 7. Forecasted commercial static density diagram.

4.2. Measures for the Development of Commercial Space

(1) Multi-center development

According to the optimization results, commercial space in Weinan City's center should be developed in a multi-center cluster, forming a spatial layout of "one primary and two secondary" centers, as illustrated in Figure 8.

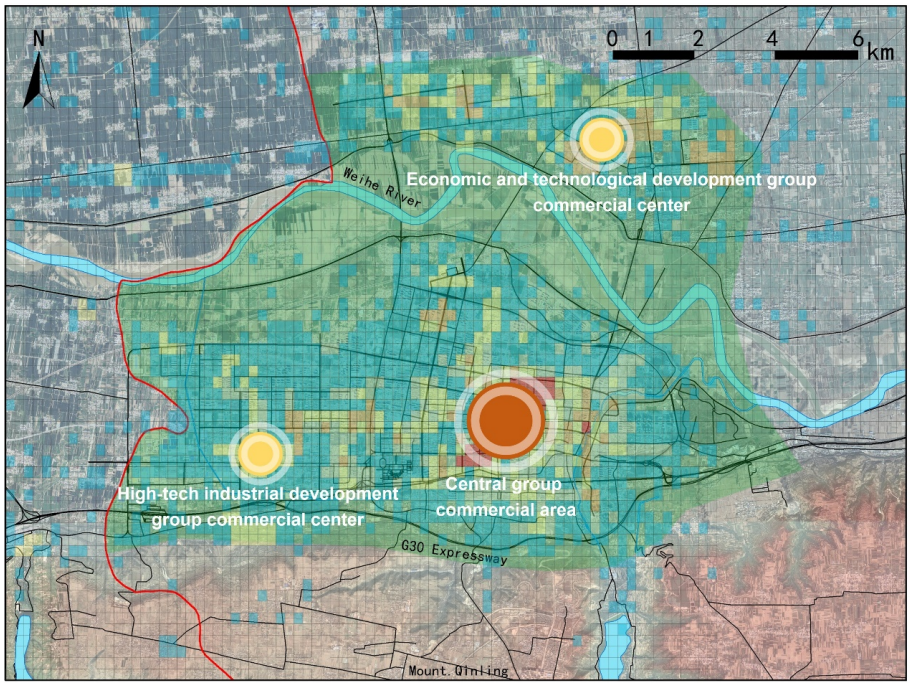

Figure 8. Multi-center space layout diagram.

The "primary" refers to the central group commercial area, which should continue along its current development trajectory, enhance the quality of its regional commercial facilities, and play a core driving role.

The "secondary" centers consisted of the high-tech industrial development group commercial center and the economic and technological development group commercial center. The high-tech industrial development group commercial center was located in the high-tech industrial development zone, in proximity to Xi'an City, and was a significant layout area for the integration and development of Xi'an and Weinan Cities. The high-tech industrial development group should revolve around Wanda Plaza, continuously improving commercial facilities to spur the development of regional commercial space.

The economic and technological development group, which was located on the north bank of the Weihe River, should focus on enterprise-centered commercial facilities, enhance the degree of commercial facility aggregation, and establish a new commercial sub-center to drive the development of commercial space within the economic and technological development zone.

(2) Multi-axis development

According to the optimization results, commercial space in Weinan City's center should adopt a "primary and secondary" spatial layout along the development axes. Figure 9 illustrates these two development axes: one extending northward from the central group, and the other westward.

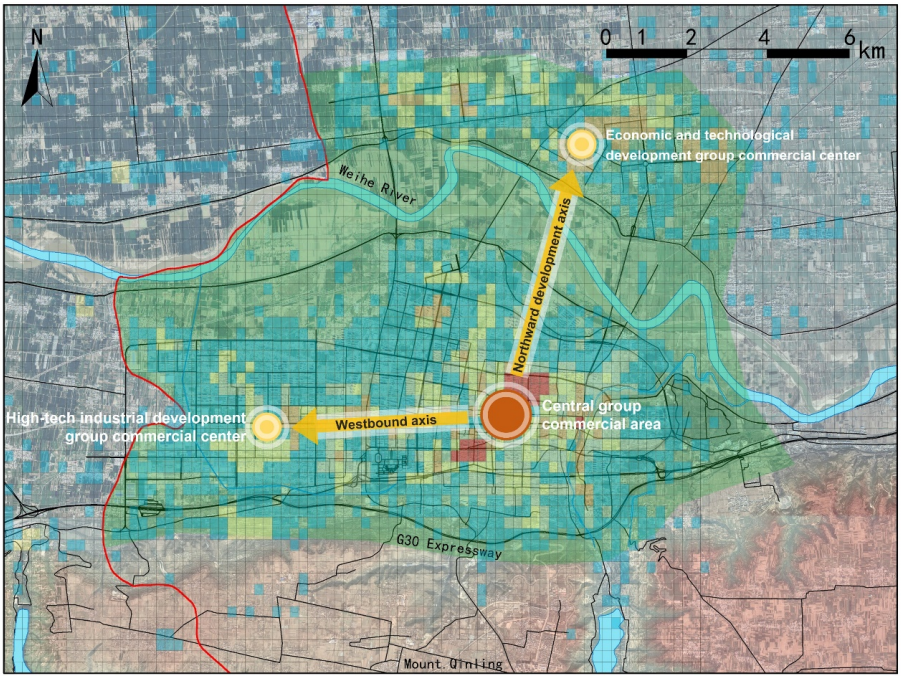

Figure 9. Axis development diagram.

Commercial space development in central Weinan should primarily follow the westward axis, given its superior infrastructure environment and rapid expansion rate. Prioritizing the westward development axis can also accelerate the integration process between Xi'an and Weinan City, which aligns with the planning of the Xi'an metropolitan area.

While the region north of the central group possessed abundant land resources, especially across the Weihe River, its slower development rate made it a more suitable secondary development axis. Although the development of commercial space across the river is an inevitable trend, this area should serve as a complement to the main westward development axis.

(3) Office space guides business development

The results from related studies show that the strongest correlation between the office function POI data and commercial function POI data occurred in Weinan City's central urban area. This suggests that areas with a concentration of office spaces should also be the

sites for commercial facilities. Thus, when planning commercial space development, the central area of Weinan City should prioritize aligning with office spaces. This approach is both effective and sensible.

As demonstrated in Figure 10, there was a considerable overlap between the concentration of office spaces and commercial spaces in the central cluster. This overlap will further enhance the densification of commercial spaces. Meanwhile, in the high-tech industrial development and the economic and technological development clusters, the office and commercial spaces were somewhat distanced from each other. In these areas, the expansion of commercial spaces should progressively move toward office spaces.

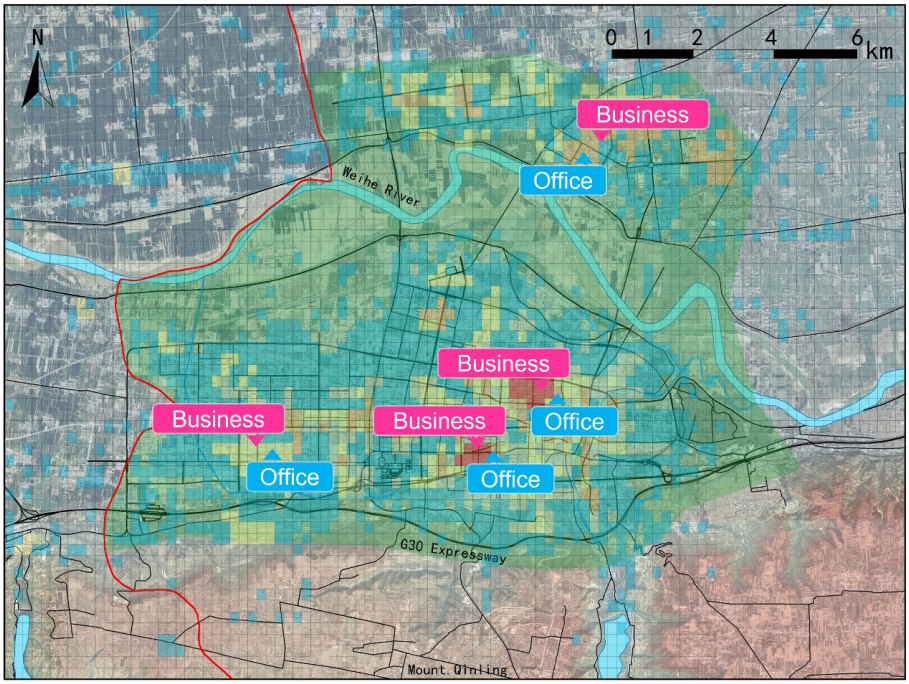

Figure 10. Space guide diagram.

5. Conclusions

The BP neural network algorithm, which was based on POI big data, was leveraged to optimize the expansion of commercial space in the central urban area of Weinan City. This study revealed key insights that significantly contribute to urban development and commercial spatial planning research.

1. This study, which dissected the city into 1097 grid cells, utilized a sophisticated machine learning model to refine the commercial landscape, yielding an R^2 value of 0.7046. The optimization effectively increased the number of commercial facilities from 44,034 to 49,871, showcasing a marked progression in urban commercial optimization. This positive trajectory underscored the viability and reliability of the data-driven approach taken in research, thereby enriching the corpus of urban planning literature with practical, data-backed insights for spatial planning.
2. Conforming to established urban economic theories, such as agglomeration theory and central place theory, this study's results delineated two principal clusters of commercial agglomeration within the city's downtown. The preferential expansion to the north and west delineated a targeted direction for future commercial space development, reflecting a broader pattern of urban spatial growth favoring agglomeration economies. These outcomes not only resonate with previous findings in urban spatial studies but also highlight the relevance of theoretical frameworks in decoding the complexities of commercial space distribution.

3. This research suggests a three-tiered optimization strategy for the commercial space in Weinan City's center, encompassing spatial structuring, a development trajectory, and regulatory guidelines. It envisions a multi-centered spatial structure, advocates for a multi-directional development axis, and prescribes adherence to a principle where office space developments precede and inform commercial space expansions. This holistic strategy offers novel insights into urban commercial space dynamics, proposing a synchronized approach to commercial and office space development.

In summary, the commercial landscape in Weinan City's center is poised for growth, with an emphasis on multi-centric and multi-axis development strategies that are energized with the progression of office spaces. The insights garnered from this study significantly contribute to the formulation of nuanced urban commercial development plans and enhance the scholarly understanding of urban commercial space evolution.

However, this study was not without its limitations. The reliance on current POI data may not fully account for future changes in urban dynamics, including evolving economic conditions and policy shifts. Further research is needed to incorporate predictive models that account for these variables and to explore the interplay between commercial space development and other urban factors, such as residential patterns and public amenities. Future investigations could also expand upon the integration of real-time data analytics and the exploration of adaptive planning strategies that can dynamically respond to urban growth patterns. These avenues will continue to refine the precision of urban planning and contribute to the sustainable development of urban commercial spaces.

Author Contributions: Conceptualization, D.Y. and J.Z.; methodology, D.Y.; software, J.Z.; validation, D.Y., J.Z. and P.X.; formal analysis, D.Y.; investigation, J.Z.; resources, P.X.; data curation, J.Z.; writing—original draft preparation, J.Z.; writing—review and editing, D.Y.; visualization, P.X.; supervision, D.Y.; project administration, D.Y.; funding acquisition, D.Y. All authors have read and agreed to the published version of the manuscript.

Funding: This research received no external funding.

Institutional Review Board Statement: Not applicable.

Informed Consent Statement: Not applicable.

Data Availability Statement: The data presented in this study are available on request from the corresponding author.

Conflicts of Interest: The authors declare no conflicts of interest.

References

1. Ko, J.; Ennemoser, B.; Yoo, W.; Yan, W.; Clayton, M.J. Architectural spatial layout planning using artificial intelligenc. *Autom. Constr.* **2023**, *154*, 105019. [CrossRef]
2. Zhou, W.; Zhang, Y.; Li, X. Artificial intelligence, green technological progress, energy conservation, and carbon emission reduction in China: An examination based on dynamic spatial Durbin modeling. *J. Clean. Prod.* **2024**, *446*, 141142. [CrossRef]
3. Li, Z.; Ma, J.; Jiang, F.; Zhang, S.; Tan, Y. Assessing the impacts of urban morphological factors on urban building energy modeling based on spatial proximity analysis and explainable machine learning. *J. Build. Eng.* **2024**, *85*, 108675. [CrossRef]
4. Lin, L.; Di, L.; Zhang, C.; Guo, L.; Zhao, H.; Islam, D.; Li, H.; Liu, Z.; Middleton, G. Modeling urban redevelopment: A novel approach using time-series remote sensing data and machine learning. *Geogr. Sustain.* **2024**, *5*, 211–219. [CrossRef]
5. Wang, Z.; Wang, X.; Dong, Z.; Li, L.; Li, W.; Li, S. More Urban Elderly Care Facilities Should Be Placed in Densely Populated Areas for an Aging Wuhan of China. *Land* **2023**, *12*, 220. [CrossRef]
6. Yang, X.; Pu, F. Spatial Cognitive Modeling of the Site Selection for Traditional Rural Settlements: A Case Study of Kengzi Village, Southern China. *J. Urban Plan. Dev.* **2020**, *146*, 25–28. [CrossRef]
7. Zhang, Y.; Zhang, Q.; Zhao, Y.; Deng, Y.; Zheng, H. Urban spatial risk prediction and optimization analysis of POI based on deep learning from the perspective of an epidemic. *Int. J. Appl. Earth Obs. Geoinf.* **2022**, *112*, 102942. [CrossRef] [PubMed]
8. Wang, R.; Feng, Z.; Pearce, J.; Yao, Y.; Li, X.; Liu, Y. The distribution of green space quantity and quality and their association with neighbourhood socioeconomic conditions in Guangzhou, China: A new approach using deep learning method and street view images. *Sustain. Cities Soc.* **2020**, *66*, 102664. [CrossRef]
9. Babahajiani, P.; Fan, L.; Kämäräinen, J.-K.; Gabbouj, M. Urban 3D segmentation and modelling from street view images and LiDAR point clouds. *Mach. Vis. Appl.* **2017**, *28*, 679–694. [CrossRef]

10. Mazhar, T.; Irfan, H.M.; Haq, I.; Ullah, I.; Ashraf, M.; Shloul, T.A.; Ghadi, Y.Y.; Imran; Elkamchouchi, D.H. Analysis of Challenges and Solutions of IoT in Smart Grids Using AI and Machine Learning Techniques: A Review. *Electronics* **2023**, *12*, 242. [CrossRef]
11. Alwahedi, F.; Aldhaheri, A.; Ferrag, M.A.; Battah, A.; Tihanyi, N. Machine learning techniques for IoT security: Current research and future vision with generative AI and large language models. *Internet Things Cyber-Phys. Syst.* **2024**, *4*, 167–185. [CrossRef]
12. Mehra, N.; Swain, J.B. Assessment of land use land cover change and its effects using artificial neural network-based cellular automation. *J. Eng. Appl. Sci.* **2024**, *71*, 70. [CrossRef]
13. Ouma, Y.O.; Nkwae, B.; Odirile, P.; Moalafhi, D.B.; Anderson, G.; Parida, B.; Qi, J. Land-Use Change Prediction in Dam Catchment Using Logistic Regression-CA, ANN-CA and Random Forest Regression and Implications for Sustainable Land–Water Nexus. *Sustainability* **2024**, *16*, 1699. [CrossRef]
14. Yao, Y.; Zhou, K.; Liu, C.; Sun, Z.; Chen, D.; Li, L.; Cheng, T.; Guan, Q. Temporal-VCA: Simulating urban land use change using coupled temporal data and vector cellular automata. *Cities* **2024**, *149*, 104975. [CrossRef]
15. Wang, H.; Xue, H.; Yang, Y.; He, W.; Liu, S.; Zhong, Y.; Gao, X.; Xu, T. Multi-Scenario Simulation and Eco-Environmental Effects Analysis of Land Use/Cover Change in China by an Integrated Cellular Automata and Markov Model. *Land* **2024**, *13*, 520. [CrossRef]
16. Liu, M.; Luo, Q.; Wang, J.; Sun, L.; Xu, T.; Wang, E. VST-PCA: A Land Use Change Simulation Model Based on Spatiotemporal Feature Extraction and Pre-Allocation Strategy. *ISPRS Int. J. Geo-Inf.* **2024**, *13*, 100. [CrossRef]
17. Pantic, I.; Paunovic, J.; Cumic, J.; Valjarevic, S.; Petroianu, G.A.; Corridon, P.R. Artificial neural networks in contemporary toxicology research. *Chem.-Biol. Interact.* **2023**, *369*, 110269. [CrossRef] [PubMed]
18. Bukhtoyarov, V.V.; Tynchenko, V.S.; Nelyub, V.A.; Masich, I.S.; Borodulin, A.S.; Gantimurov, A.P. A Study on a Probabilistic Method for Designing Artificial Neural Networks for the Formation of Intelligent Technology Assemblies with High Variability. *Electronics* **2023**, *12*, 215. [CrossRef]
19. Rustamov, J.; Rustamov, Z.; Zaki, N. Green Space Quality Analysis Using Machine Learning Approaches. *Sustainability* **2023**, *15*, 7782. [CrossRef]
20. Owusu, M.; Engstrom, R.; Thomson, D.; Kuffer, M.; Mann, M.L. Mapping Deprived Urban Areas Using Open Geospatial Data and Machine Learning in Africa. *Urban Sci.* **2023**, *7*, 116. [CrossRef]
21. Roy, A.; Chakraborty, S. Support vector machine in structural reliability analysis: A review. *Reliab. Eng. Syst. Saf.* **2023**, *233*, 109126. [CrossRef]
22. Li, S.; Chen, H.; Chen, Y.; Xiong, Y.; Song, Z. Hybrid Method with Parallel-Factor Theory, a Support Vector Machine, and Particle Filter Optimization for Intelligent Machinery Failure Identification. *Machines* **2023**, *11*, 837. [CrossRef]
23. Yang, D.; Zhao, J.; Suhail, S.A.; Ahmad, W.; Kamiński, P.; Dyczko, A.; Salmi, A.; Mohamed, A. Investigating the Ultrasonic Pulse Velocity of Concrete Containing Waste Marble Dust and Its Estimation Using Artificial Intelligence. *Materials* **2022**, *15*, 4311. [CrossRef] [PubMed]
24. Zhang, M.; Millar, M.-A.; Chen, S.; Ren, Y.; Yu, Z.; Yu, J. Enhancing hourly heat demand prediction through artificial neural networks: A national level case study. *Energy AI* **2024**, *15*, 100315. [CrossRef]
25. Peng, S.; Tan, J.; Ma, H. Carbon emission prediction of construction industry in Sichuan Province based on the GA-BP model. *Environ. Sci. Pollut. Res.* **2024**, *31*, 24567–24583. [CrossRef] [PubMed]
26. Goel, A.; Goel, A.K.; Kumar, A. The role of artificial neural network and machine learning in utilizing spatial information. *Spat. Inf. Res.* **2023**, *31*, 275–285. [CrossRef]
27. Gautam, V.K.; Pande, C.B.; Moharir, K.N.; Varade, A.M.; Rane, N.L.; Egbueri, J.C.; Alshehri, F. Prediction of Sodium Hazard of Irrigation Purpose using Artificial Neural Network Modelling. *Sustainability* **2023**, *15*, 7593. [CrossRef]
28. Li, L.; Ren, X. A Novel Evaluation Model for Urban Smart Growth Based on Principal Component Regression and Radial Basis Function Neural Network. *Sustainability* **2019**, *11*, 6125. [CrossRef]
29. Li, C.; Gao, X.; Wu, J.; Wu, K. Demand prediction and regulation zoning of urban-industrial land: Evidence from Beijing-Tianjin-Hebei Urban Agglomeration, China. *Environ. Monit. Assess* **2019**, *191*, 412. [CrossRef]
30. Karamouz, M.; Kia, M.; Nazif, S. Prediction of Sea Level Using a Hybrid Data-Driven Model: New Challenges after Hurricane Sandy. *Water Qual. Expo. Health* **2014**, *6*, 63–71. [CrossRef]
31. Velichko, A.; Heidari, H. A Method for Estimating the Entropy of Time Series Using Artificial Neural Networks. *Entropy* **2021**, *23*, 1432. [CrossRef] [PubMed]
32. Jin, H. Prediction of direct carbon emissions of Chinese provinces using artificial neural networks. *PLoS ONE* **2021**, *16*, e0236685. [CrossRef] [PubMed]
33. Zhao, X.; Song, M.; Liu, A.; Wang, Y.; Wang, T.; Cao, J. Data-Driven Temporal-Spatial Model for the Prediction of AQI in Nanjing. *J. Artif. Intell. Soft Comput. Res.* **2020**, *10*, 255–270. [CrossRef]
34. Zhao, J.; Jin, J.; Xu, J.; Guo, Q.; Hang, Q.; Chen, Y. Risk assessment of flood disaster and forewarning model at different spatial-temporal scales. *Theor. Appl. Clim.* **2018**, *132*, 791–808. [CrossRef]
35. Lindsay, G.W. Grounding neuroscience in behavioral changes using artificial neural networks. *Curr. Opin. Neurobiol.* **2024**, *84*, 102816. [CrossRef] [PubMed]
36. Biazar, S.M.; Shehadeh, H.A.; Ghorbani, M.A.; Golmohammadi, G.; Saha, A. Soil temperature forecasting using a hybrid artificial neural network in Florida subtropical grazinglands agro-ecosystems. *Sci. Rep.* **2024**, *14*, 1535. [CrossRef] [PubMed]

37. Peng, F.; Chen, X. An Efficient Optimization Method for Antenna Arrays Using a Small Population Diploid Genetic Algorithm Based on Local RBF Networks. *IEEE Trans. Antennas Propag.* **2024**, *72*, 3237–3249. [CrossRef]
38. Chen, H.; Liang, Y.; Huang, H.; Huang, Q.; Gu, W.; Liang, H. Live Pig-Weight Learning and Prediction Method Based on a Multilayer RBF Network. *Agriculture* **2023**, *13*, 253. [CrossRef]
39. Rubio, J.d.J.; Garcia, D.; Sossa, H.; Garcia, I.; Zacarias, A.; Mujica-Vargas, D. Energy processes prediction by a convolutional radial basis function network. *Energy* **2023**, *284*, 128470. [CrossRef]
40. Tsoulos, I.G.; Charilogis, V. Locating the Parameters of RBF Networks Using a Hybrid Particle Swarm Optimization Method. *Algorithms* **2023**, *16*, 71. [CrossRef]
41. Hernández-Luquin, F.; Escalante, H.J. Multi-branch deep radial basis function networks for facial emotion recognition. *Neural Comput. Applic.* **2023**, *35*, 18131–18145. [CrossRef]
42. Mokarram, M.; Taripanah, F.; Pham, T.M. Spatial-Temporal Analysis of Atmospheric Environment in Urban Areas using Remote Sensing and Neural Networks. *Sustain. Comput. Inform. Syst.* **2024**, *42*, 100987. [CrossRef]
43. Chiu, S.M.; Liou, Y.S.; Chen, Y.C.; Lee, C.; Shang, R.K.; Chang, T.Y.; Zimmermann, R. Universal Transfer Framework for Urban Spatio-Temporal Knowledge Based on Radial Basis Function. *IEEE Trans. Artif. Intell.* **2024**, *1*, 1–11. [CrossRef]
44. Wu, Y.; Zheng, S.; Liu, Q.; Dong, A.; Li, Q. Structural and empirical knowledge driven multi-objective evolutionary algorithm for urban drainage system design. *Expert Syst. Appl.* **2024**, *249*, 123461. [CrossRef]
45. Jaanaa Rubavathy, S.; Sungeetha, D.; Carmel Mary Belinda, M.J.; Jayant, G.; Emad, K.; Hitesh, P.; Gomathi, S.; Deepa, P.; Aravind Kumar, J.; Praveenkumar, T.R. An inimitable Elman network based fire hawk controller and skill optimized power tracker with ultra gain converter for improving the performance of PV tied EV systems. *Case Stud. Therm. Eng.* **2024**, *56*, 104183. [CrossRef]
46. Bhatti, M.A.; Song, Z.; Bhatti, U.A.; Syam, S.M. AIoT-driven multi-source sensor emission monitoring and forecasting using multi-source sensor integration with reduced noise series decomposition. *J. Cloud Comp.* **2024**, *13*, 65. [CrossRef]
47. Ebenezer, P.A.; Manohar, S. Land use/land cover change classification and prediction using deep learning approaches. *SIViP* **2024**, *18*, 223–232. [CrossRef]
48. Liu, X.-S.; Deng, Z.; Wang, T.-L. Real estate appraisal system based on GIS and BP neural network. *Trans. Nonferrous Met. Soc. China* **2011**, *21*, s626–s630. [CrossRef]
49. He, B.; Bai, M.; Liu, B.; Li, P.; Qiu, S.; Li, X.; Ding, L. Evaluation of Drifting Snow Susceptibility Based on GIS and GA-BP Algorithms. *ISPRS Int. J. Geo-Inf.* **2022**, *11*, 142. [CrossRef]
50. Wang, Y.; Wang, N.; Zhao, X.; Liang, X.; Liu, J.; Yang, P.; Wang, Y.; Wang, Y. Field Model-Based Cultural Diffusion Patterns and GIS Spatial Analysis Study on the Spatial Diffusion Patterns of Qijia Culture in China. *Remote Sens.* **2022**, *14*, 1422. [CrossRef]
51. Wu, L.; Zhang, Y.; Wei, Y.; Chen, F. A BP Neural Network-Based GIS-Data-Driven Automated Valuation Framework for Benchmark Land Price. *Complexity* **2022**, *2022*, 1695265. [CrossRef]
52. Huang, L.; Xie, G.; Zhao, W.; Gu, Y.; Huang, Y. Regional logistics demand forecasting: A BP neural network approach. *Complex Intell. Syst.* **2023**, *9*, 2297–2312. [CrossRef]
53. Bentivoglio, R.; Isufi, E.; Jonkman, S.N.; Taormina, R. Deep learning methods for flood mapping: A review of existing applications and future research directions. *Hydrol. Earth Syst. Sci.* **2022**, *26*, 4345–4378. [CrossRef]
54. Alonso, L.; Zhang, Y.R.; Grignard, A.; Noyman, A.; Sakai, Y.; ElKatsha, M.; Doorley, R.; Larson, K. CityScope: A Data-Driven Interactive Simulation Tool for Urban Design. Use Case Volpe. In *Unifying Themes in Complex Systems IX. ICCS 2018*; Morales, A., Gershenson, C., Braha, D., Minai, A., Bar-Yam, Y., Eds.; Springer Proceedings in Complexity; Springer: Cham, Switzerland, 2018. [CrossRef]
55. Li, Y.-W.; Cao, K. Establishment and application of intelligent city building information model based on BP neural network model. *Comput. Commun.* **2020**, *153*, 382–389. [CrossRef]
56. LeCun, Y.; Bengio, Y.; Hinton, G. Deep learning. *Nature* **2015**, *521*, 436–444. [CrossRef] [PubMed]
57. Ganin, Y.; Ustinova, E.; Ajakan, H.; Germain, P.; Larochelle, H.; Laviolette, F.; Marchand, M.; Lempitsky, V. Domain-Adversarial Training of Neural Networks. *J. Mach. Learn. Res.* **2016**, *17*, 1–35.
58. Mohamed, A.R.; Dahl, G.E.; Hinton, G. Acoustic modeling using deep belief networks. *IEEE Trans. Audio Speech Lang. Process.* **2011**, *20*, 14–22. [CrossRef]
59. Yamashita, R.; Nishio, M.; Do, R.K.G.; Togashi, K. Convolutional neural networks: An overview and application in radiology. *Insights Imaging* **2018**, *9*, 611–629. [CrossRef] [PubMed]
60. Nafisah, S.I.; Muhammad, G. Tuberculosis detection in chest radiograph using convolutional neural network architecture and explainable artificial intelligence. *Neural Comput. Applic.* **2024**, *36*, 111–131. [CrossRef] [PubMed]
61. Mokri, S.M.G.; Valadbeygi, N.; Stelnikova, I.G. Using Convolutional Neural Network to Design and Predict the Forces and Kinematic Performance and External Rotation Moment of the Hip Joint in the Pelvis. *Int. J. Innov. Sci. Res. Technol. (IJISRT)* **2024**, *IJISRT24FEB1059*, 878–883. [CrossRef]
62. Wang, J.; Wang, Y.; Li, C.; Li, Y.; Qi, H. Landslide susceptibility evaluation based on landslide classification and ANN-NFR modelling in the Three Gorges Reservoir area, China. *Ecol. Indic.* **2024**, *160*, 111920. [CrossRef]
63. Faruk, D.Ö. A hybrid neural network and ARIMA model for water quality time series prediction. *Eng. Appl. Artif. Intell.* **2010**, *23*, 586–594. [CrossRef]
64. Sherstinsky, A. Fundamentals of recurrent neural network (RNN) and long short-term memory (LSTM) network. *Phys. D Nonlinear Phenom.* **2020**, *404*, 132306. [CrossRef]

65. Javed, A.; Kim, T.; Lee, C.; Oh, J.; Han, Y. Deep learning-based detection of urban forest cover change along with overall urban changes using very-high-resolution satellite images. *Remote Sens.* **2023**, *15*, 4285. [CrossRef]
66. Zhang, Z.; Wang, H.; Xu, F.; Jin, Y.Q. Complex-valued convolutional neural network and its application in polarimetric SAR image classification. *IEEE Trans. Geosci. Remote Sens.* **2017**, *55*, 7177–7188. [CrossRef]
67. Goyal, M.K.; Bharti, B.; Quilty, J.; Adamowski, J.; Pandey, A. Modeling of daily pan evaporation in sub tropical climates using ANN, LS-SVR, Fuzzy Logic, and ANFIS. *Expert Syst. Appl.* **2014**, *41*, 5267–5276. [CrossRef]
68. Talaei Khoei, T.; Ould Slimane, H.; Kaabouch, N. Deep learning: Systematic review, models, challenges, and research directions. *Neural Comput. Appl.* **2023**, *35*, 23103–23124. [CrossRef]
69. Francini, M.; Salvo, C.; Vitale, A. Combining deep learning and multi-source GIS methods to analyze urban and greening changes. *Sensors* **2023**, *23*, 3805. [CrossRef] [PubMed]
70. Aljarah, I.; Faris, H.; Mirjalili, S. Optimizing connection weights in neural networks using the whale optimization algorithm. *Soft Comput.* **2018**, *22*, 1–15. [CrossRef]